Biosensors and Bioelectronics 61 (2014) 598–604

Contents lists available at ScienceDirect

Biosensors and Bioelectronics

journal homepage: www.elsevier.com/locate/bios

A universal lateral flow biosensor for proteins and DNAs based on the conformational change of hairpin oligonucleotide and its use for logic gate operations

Yan Huang [a], Wei Wen [a], Dan Du [b,c], Xiuhua Zhang [a], Shengfu Wang [a,*], Yuehe Lin [b,**]

[a] Hubei Collaborative Innovation Center for Advanced Organic Chemical Materials, Ministry of Education Key Laboratory for the Synthesis and Application of Organic Functional Molecules & College of Chemistry and Chemical Engineering, Hubei University, Wuhan 430062, PR China
[b] School of Mechanical and Materials Engineering, Washington State University, Pullman 99164, USA
[c] Key Laboratory of Pesticide and Chemical Biology of Ministry of Education, College of Chemistry, Central China Normal University, Wuhan 430079, PR China

ARTICLE INFO

Article history:
Received 25 February 2014
Received in revised form
22 May 2014
Accepted 3 June 2014
Available online 11 June 2014

Keywords:
Logic gates
Hairpin oligonucleotides
Strip biosensor
Gold nanoparticles

ABSTRACT

A universal lateral flow biosensor for proteins and DNAs was designed on the base of target-induced conformational changes of hairpin oligonucleotide (HO). CEA (carcinoembryonic antigen) protein and c-DNA were detected both with the naked eye and a strip reader. The scheme of detecting proteins and DNAs were based on the unique molecular recognition properties of HO to the targets to form different quantities of "active" biotin groups on the surface of gold nanoparticles (AuNPs). The output of the strip is the color of the test line, which inspired us to combine strip biosensor with logic gate. Two strip logic gates ("OR" and "INH") were designed in our paper and the combinatorial logic gates in our paper could be used to make high-throughput judgment about what targets were present in the input samples according to the output results. The biosensor facilitates a portable analysis at ambient temperature as it is simple to be conducted and no requirement of training is needed. The strip logic system is proved an excellent selection and can operate effectively as well as in human serum samples. Therefore, we indicate that such logic strips a foreseeable promise in application of intelligent point-of-care and in-field diagnostics.

1. Introduction

Molecular Boolean logic gate concept derived from electronic logic gates of conventional computer microprocessors. There is a widely accepted notion that this idea has caught many scholars' interest and inspired the generation of smart chemical and biochemical systems (Andreasson and Pischel, 2010; Chen et al., 2006; Katz and Privman, 2010) for functional materials, diagnostic and biosensing applications (Halámková et al., 2012; Vinkenborg et al., 2011; Wang et al., 2014). In the last a few years, chemical systems attained a remarkable interest from researchers and are increasingly imposed in Boolean logic operations for progress of a variety of molecule-based logic systems, such as AND, OR, XOR, NAND, NOR, INHIBIT, half-adder, and half-subtractor (Pu et al., 2011a,b; Lin et al., 2011; Liu et al., 2012; Wang et al., 2012; J. Zhang et al., 2013; L. Zhang et al., 2013; Kim et al., 2013). It could be inspiring to declare that (bio) chemical reaction systems have been in center of life reactions as same as silicon being important to computers. Cascading is supposed to perform providing the chosen substrate's output is of a same form than the input.

It is agreed by most scholars that aptamers, the artificial nucleic acid ligands, are firstly discovered by two groups in 1990 (Tuerk and Gold, 1990; Ellington and Szostak, 1990). Thereafter, aptamers have been exploited to combine with a wide range of small molecules, proteins and DNAs due to their distinct characteristics, such as the high association constant with target proteins and small molecules, easy to obtain and readily to be labelled with signal moieties, cost-effectiveness, and long-term stability (Yoshida and Yokobayashi, 2007; Pan et al., 2013). Noticeably, the combination of DNA oligonucleotides and gold nanoparticles (AuNPs) has been applied for colorimetric logic gates design (Lu et al., 2013), by taking advantage of the recognition ability of aptamers and the unique optical properties of AuNPs. It has been proved that some DNA aptamers can be split into two fragments (Liu et al., 2010; Xu et al., 2009; Zhang et al., 2008). Based on these findings, the 15-mer antithrombin aptamer and 27-mer anti-ATP

* Corresponding author. Tel.: +86 27 50865309; fax: +86 27 88663043.
** Corresponding author.
E-mail addresses: wangsf@hubu.edu.cn (S. Wang), yuehe.lin@pnl.gov (Y. Lin).

http://dx.doi.org/10.1016/j.bios.2014.06.007
0956-5663/

aptamer are split into two fragments respectively in Zeng group's recent work (Chen et al., 2012). The two fragments equilibrate between the disassociated parts and the associated complex, and can reassemble to form a ligand-stabilized structure in the presence of targets. However, this method cannot be a regular approach for potential high-transmission-efficiency substrate because it has strict requirements on target. The target aptamer have to be split into two fragments and retain the recognition ability of each domain when two fragments were integrated together. Therefore, hairpin oligonucleotides (HO) caught our attention as a substitute. It embodies a unique stem–loop structure to provide high specificity, enabling the universal, simple, rapid, and sensitive detection of any proteins and DNAs (He et al., 2010, 2012; Li et al., 2007; Niu et al., 2011; Wang et al., 2008; Zhang et al., 2010).

Recently more and more effort has been made to aim at developing point-of-care (POC) diagnosis biosensors. Strip biosensors bring an optional method for this goal and have attracted great interests for their short assay time, cost-effectiveness, portable format, and stability during long-time storage (Wang et al., 2011; Liu et al., 2011; Du et al., 2012). Moreover, complex analysis procedure brought by expensive instrumentation is avoided and highly qualified personnel are not necessary. Zeng's group has successfully developed LFSB for the detection of nucleic acids (Lie et al., 2012; Liu et al., 2013), proteins (Fang et al., 2011; Ge et al., 2013), cancer cells (Liu et al., 2009), and heavy metal ions (Fang et al., 2010). The detection outcome is easy to perform by visually observing the color intensity of the red band on the test line. Furthermore, the quantitative data can be collected by recording the optical replies with a portable "strip reader". For the purpose of searching new orientations in molecular logic gates, it would be of great importance to incorporate strips with logic gates. Herein, we report a universal hairpin oligonucleotide system established for visual and sensitive detection of proteins and DNAs as well as a pair of strip logic gates that regard the red band on the test line of LFSB as outputs in response to a protein and a DNA, CEA (carcinoembryonic antigen) protein and c-DNA.

2. Experimental

2.1. Chemicals and materials

Streptavidin (SA), hydrogen tetrachloroaurate (III) trihydrate ($HAuCl_4 \cdot 3H_2O$), trisodium citrate, sucrose, Tween-20, Triton X-100, Tris(2-carboxyethyl)phosphine (TCEP), dATP (deoxyadenosine triphosphate), bovine serum albumin (BSA), CEA from human fluids ($\geq$95%, SDS-PAGE), human serum were purchased from Sigma-Aldrich (USA). Nitrocellulose membrane (HFB18004) was purchased from Millipore (Billerica, MA). Polyester fiber (VL78), laminated cards (SM31-40), HM3030 dispenser, CTD300P programmable strip cutter, DT2032 portable strip reader were purchased from Shanghai Kinbio Tech. Co., Ltd. Shanghai, China. Hairpin oligonucleotide, target DNA and control DNA probe were synthesized and purified by Sangon (Shanghai, China). The oligonucleotide sequences were as follows:

CEA-HO: 5′-HS-$(CH_2)_6$-CCA CgA TAC CAg CTT ATT CAA TTC gTg g-biotin-3′

DNA-HO: 5′-HS-$(CH_2)_6$-ACA Cgg CAg TTg ATC CTT Tgg ATA CCC Tgg CgT gT-biotin-3′

OTA-HO: 5′-HS-$(CH_2)_6$-TTT TTg ATC ggg TgT ggg Tgg CgT AAA ggg AgC ATC ggA CAA AAA A-biotin-3′

c-DNA: 5′-CCA ggg TAT CCA AAg gAT CAA CTg C-3′

1m-DNA: 5′-CCA ggg TAT CCA ACg gAT CAA CTg C-3′

3m-DNA: 5′-CCA ggg TAT gCg ACg gAT CAA CTg C-3′

All chemicals used in this study were analytical reagent grade. All other solutions were prepared with ultrapure (18.2 M cm^{-1}) water from a Millipore Milli-Q water purification system (Billerica, MA).

2.2. Preparation of gold nanoparticles (AuNPs)

AuNPs with diameter 15 ± 3.5 nm were prepared regarding to the reported methods with slight modifications (Mao et al., 2009). All glassware applied in this preparation was completely cleaned in aqua regia (three parts HCl and one part HNO_3), rinsed in doubly distilled water, and oven-dried prior to use. In a 250 mL conical flask, 100 mL of 0.01% $HAuCl_4$ in ultrapure water were heated to boil with vigorous stirring, followed by the addition of

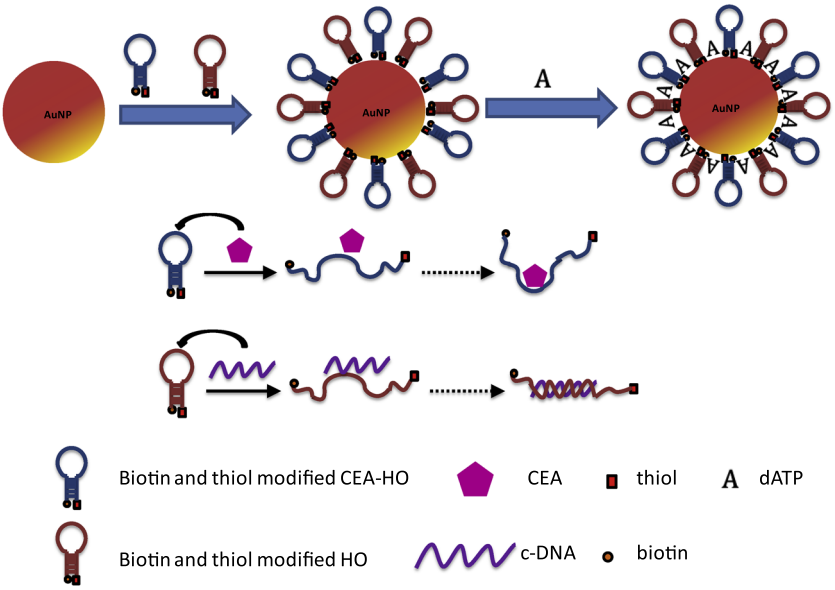

Scheme 1. Schematic illustration for preparation of DNA–AuNPs conjugates and conformational switch of HO.

4 mL of 1% trisodium citrate. The solution turned deep blue within 20 s, and the final color changed to wine-red after 60 s. Boiling state last for an additional 10 min; the heating source was removed, and the colloid solution was stirred for another 15 min. The resulting AuNPs solution was stored in dark bottles at 4 °C and used to prepare the HO–AuNPs conjugate.

2.3. Preparation of DNA–AuNPs conjugates

HO modified with a thiol at its 5′ end and biotin at its 3′ end was imposed to synthesize HO–AuNP compound (Scheme 1). 5 μL 10 μM of CEA-HO, 5 μL 10 μM of DNA–HO and 5 μL 1 mM TCEP were added to 250 μL of the 10-fold concentrated AuNPs solution to prepare OR–DNA–AuNPs. After shaking 1 h at room temperature (RT), 50 μL of 14.1 μM dATP were attached to the solution and shook 30 min at RT. The HO–AuNP conjugates were incubated for half an hour at RT and then put at 4 °C for 4 h to continue increasing the stability of the conjugate. The excess reagents were removed by centrifugation for 8 min at 12,000 rpm. After discarding the supernatant, the red pellets were washed twice with 10 mM PBSB (pH 7.4, 1% BSA), with the centrifugation time of 13 min at 12,000 rpm; recentrifuged; redispersed in 300 μL of an aqueous solution containing 20 mM $Na_3PO_4 \cdot 12H_2O$, 5% BSA, 0.25% Tween, and 10% sucrose; and stored at 4 °C before further use. INH–DNA–AuNPs were provided with a slight change, which was carried out by adding 5 μL 10 μM of CEA-HO and 5 μL 1 mM TCEP to 250 μL of the 10-fold concentrated AuNPs solution. Other procedures were done the same way as in the OR–DNA–AuNPs conjugation reactions.

The 10 μM solution of the HOs were prepared in the buffer [Tris–HCl (20 mM, pH 7.4), 100 mM NaCl, and 5 mM $MgCl_2 \cdot 6H_2O$]. The solution was incubated at 95 °C for 5 min and then allowed to slowly cool to RT over 30 min so that the probe correctly folded into a hairpin structure. TCEP, a thiol deoxidizer, was used to shear the disulfide bond formed between the thiol groups. dATP, a monomer unit of nucleic acid, was used as a blocker to prepare the DNA–AuNP conjugates.

2.4. Preparation of the strips

Three components consisting of the sample pad, nitrocellulose membrane, and absorbent pad were pasted on a common backing layer (typically an inert plastic, e.g., polyester). The material of the sample pad was selected as a kind of polyester fiber and its size is 29 mm × 30 cm. It was saturated with a buffer (pH 8.0) containing 0.25% Triton X-100, 0.02 M Tris–HCl, and 0.15 M NaCl for 1 h, then dried at 37 °C for 2 h and at last stored in desiccators at RT before use. A concentration of 2 mg mL^{-1} streptavidin and 2 mg mL^{-1} streptavidin–biotinylated control DNA probe solutions were respectively dispensed on the nitrocellulose membrane as test line and control line (CT) with the HM3030 dispenser (Shanghai Kinbio Tech. Co., Ltd. Shanghai, China). The size of the nitrocellulose membrane is 25 mm × 30 cm. They would be easily washed away by the sample solution if control DNA probes are directly dispensed on the nitrocellulose membrane. Therefore, streptavidin was utilized to combine with the biotinylated control DNA probes to form the streptavidin–biotin DNA conjugates so that control DNA probes could be immobilized on the nitrocellulose membrane. The space between the test line and control line was set as 5 mm. The membrane was dried at 4 °C before use. Finally, following by fabricating the nitrocellulose membrane on a plastic adhesive backing (80 mm × 30 cm), the sample pad and absorption pad were fabricated with 2 mm overlapped to facilitate migration of the solution on the strip in time of the assay. Instead of choosing a conjugate pad to store DNA–AuNPs conjugates, we put them in centrifuge tubes at 4 °C before use.

2.5. Assay procedure

Different concentrations of CEA (0, 1, 10, 50, 100, 200 ng mL^{-1}) or c-DNA (0, 0.01, 0.1, 0.25, 0.5, 1 μM) were added to the sample solution containing 10 μL of the as-prepared OR–AuNPs conjugates. The sample solution was fixed by a running buffer (20 mM Tris–HCl, 100 mM NaCl, 5 mM $MgCl_2$, pH 7.4). The mixture was incubated for 30 min at RT and then implemented to the sample pad of the LFSB. 4 min after applying sample solution to sample pad, the biosensor was washed twice by adding 40 μL of Tris–HCl buffer on the sample pad at 3-min intervals. The red bands were observed in about 10 min. CEA and c-DNA could be both detected by our naked eye and a portable strip reader. We also evaluated different concentrations of CEA-HO at a certain amount of CEA in order to ensure the functions of the following logic gate.

2.6. Logic gates operation

For the “OR” logic gate operation, 10 μL of the as-prepared OR–AuNPs conjugates were mixed with 40 μL sample solution which contains suitable concentrations of CEA and/or c-DNA. The mixture was incubated for 30 min at RT and then implemented to the sample pad of the LFSB. 4 min after applying sample solution to sample pad, the biosensor was washed twice by adding 40 μL of Tris–HCl buffer on the sample pad at 3-min intervals. The red bands were observed in about 10 min. If there are two red bands (one is on the test line and the other is on the control line), it indicated the result is “true” (yield = 1); if there is only one red band (on the control line), it indicated the result is “false” (yield = 0). The portable “strip reader” DT2032 equipped with the “GoldBio strip reader” software (Shanghai Kinbio Tech. Co., Ltd. Shanghai, China) was used to record the grayscales of the red bands on the test and control lines. The software could turn the grayscales of the red bands to quantification parameters, peak height and peak area.

For the “INH” logic gate operation, suitable concentrations of CEA and/or CEA-HO were first added to 30 μL of Tris–HCl sample solution for 30 min. Then 10 μL of the as-prepared INH–AuNPs conjugates were mixed with 30 μL of Tris–HCl sample solution which contains appropriate concentrations of CEA and/or CEA-HO. The mixture was incubated for 30 min at RT and then implemented to the sample pad of the LFSB. Other procedures were done the same way as in the “OR” logic gate operation.

3. Results and discussion

The scheme of detecting proteins and DNAs were based on the unique molecular recognition properties of HO to the targets to form different quantities of “active” biotin groups on the AuNP surface. The HO modified with a thiol at its 5′ end and biotin at its 3′ end were immobilized onto AuNP surface through a self-assembling process. Under an embedding step by dATP (deoxyadenosine triphosphate), the biotin groups are blocked by the stem–loop structure of HO and dATP, resulting in “inactive” biotins. The scheme of detecting proteins and DNAs were based on the unique molecular recognition properties of HO to the targets to form different quantities of “active” biotin groups on the AuNP surface. After recognition reactions, the AuNPs associated with the activated biotins are captured on the test line (TL) of Lateral Flow Strip Biosensor (LFSB) via the specific reaction between the activated biotin and preimmobilized streptavidin. AuNPs accumulate to produce the characteristic red bands, which enable optical detection of proteins and DNAs.

3.1. Analytical characteristics

Three components of sample pad, nitrocellulose membrane, and absorption pad compose the LFSB. Instead of choosing a conjugate pad to store DNA–AuNPs conjugates, we put them in centrifuge tubes at 4 °C before use. Supposing that a conjugate pad were used, the incubation time (< 3 min) would not be adequate for the target-induced self-assembly of the HO and the targets, which would then lower the detection sensitivity. Streptavidin and two streptavidin–biotin–control DNA (partially complementary to the corresponding loop sequences of HO) were dispensed onto the nitrocellulose membrane to form the test and control lines, respectively.

As disclosed in Figs. S1A and S2A, the grayscale of the red bands on the test zone increased with the increase of the concentration of CEA and c-DNA. When the concentration of CEA reached at 200 ng mL^{-1} and that of c-DNA reached at 1 μM, the red band on the test line can be apparently seen by our naked eye. Figs. S1B and S2B present their corresponding optical replies by tracking down the grayscale (peak height) of the red bands using a portable strip reader. The values of peak areas on the test line were figured in Figs. S1C and S2C. In the coming assays, 200 ng mL^{-1} CEA and 1 μM c-DNA were adopted as the two inputs in the logic gate operations to make sure a complete conformation change of the HO with the targets.

We also evaluated the appropriate concentrations of CEA-HO at the amount of CEA of 200 ng mL^{-1} that ensured the functions of the "INH" logic gate. In case that a competitive recognition model was employed in the "INH" logic, the more CEA-HO emerges in solution, the less signal would be attained on the test line. Our observed visual results (Fig. S3A) clarified that as CEA-HO concentrations increased in the solution, the red band on the test line decreased. It was almost invisible at the amount of CEA-HO of 1 μM when the concentration of CEA was 200 ng mL^{-1}. Fig. S3B presents their corresponding optical replies by tracking down the grayscale (peak height) of the red bands. The values of peak areas on the test line were figured in Fig. S3C. Thus 200 ng mL^{-1} CEA and 1 μM CEA-HO participated as the two inputs in the following experiments.

3.2. Design strategy of the strip "OR" logic gate

Referring to the first logic operation, a two-analyte "OR" logic gate is designed (Scheme 2). CEA and c-DNA are the two inputs, with the absence and presence of each substance defined as "0" and "1", respectively. The color of the test line is regarded as the output, with the absence and presence of a red band on the test line defined as "0" and "1", separately. AuNPs with diameter 15 ± 3.5 nm were exercised in our experiments because they are relatively small as well as stable and are able to promote the sensitivity and reproducibility of strip biosensors.

In the (0,0) state of the "OR" gate, which is in the absence of CEA and c-DNA, there was no compound, produced by the CEA and CEA-HO, or duplex DNA, hybridized by c-DNA and DNA–HO in the sample solution, the hairpin structure remained leading to the biotin still masked by the AuNP; therefore, no AuNP conjugate was captured on the test line of the LFSB, and no red band was observed in the test line. The solution migrates along the strip by capillary action and the HO–AuNP are captured on the control line because of the hybridization reactions between the streptavidin–biotin–control DNA and the loop sequences of HO, bringing about the red band in the control line. In the presence of both inputs (1,1) or in the presence of either input (1,0) (0,1), CEA and/or c-DNA combine with the loop sequences of the corresponding HO, the distinct stem–loop structure breaks down, pulls the biotin away from the AuNP surface, contributing the biotin group "active" (Scheme 1). AuNPs associated with the activated biotins are captured on the test line of LFSB via the specific reaction between the activated biotin and preimmobilized streptavidin. AuNPs accumulate to produce the characteristic red bands in the test line.

Part A of Fig. 1 shows representative photo images of the "OR" gate, part B presents corresponding peak height of the test line and control line, part C presents corresponding peak area of the test line. Comparing with no obvious phenomenon on the test line in the original state (0,0), the characteristic red bands appear when the logic circuit was employed to either or both inputs, at the same time, the peak heights are much higher and the peak areas are much larger. The results are concluded in a truth table in part D.

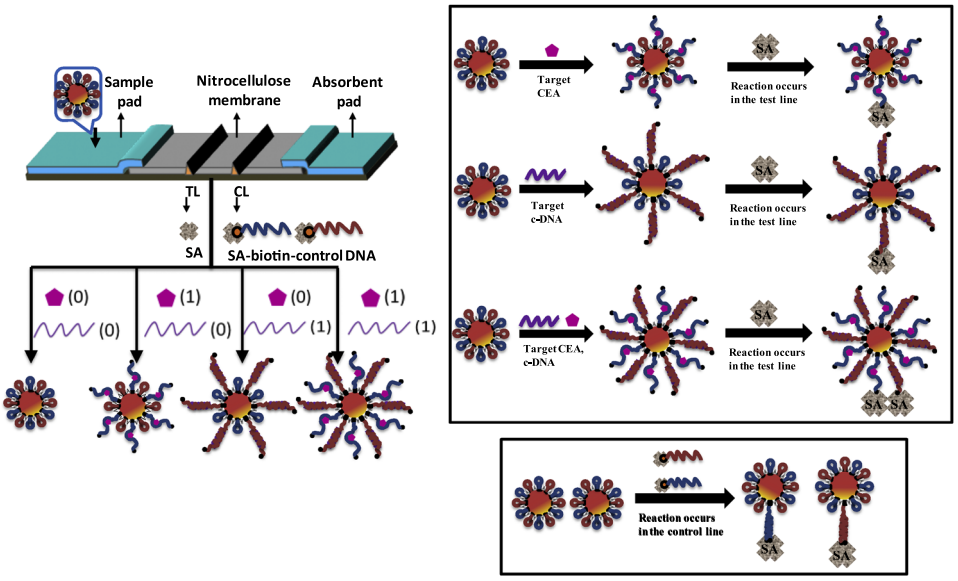

Scheme 2. Schematic illustration of the design strategy of the strip "OR" logic gate using CEA and c-DNA as inputs.

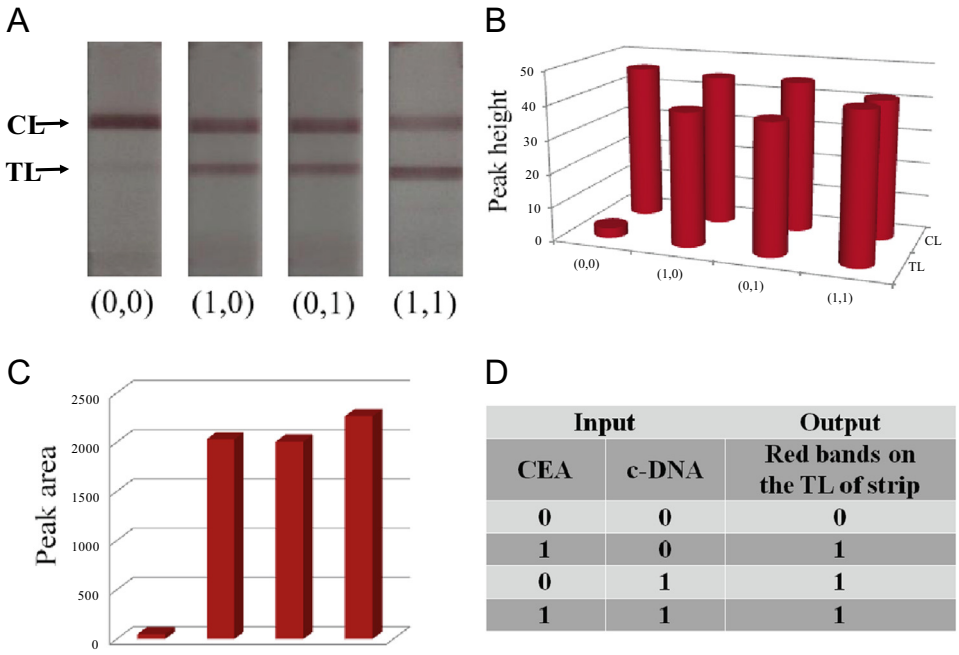

Input		Output
CEA	c-DNA	Red bands on the TL of strip
0	0	0
1	0	1
0	1	1
1	1	1

Fig. 1. (A) Photo image of the LFSB in "OR" gate. (B) Peak height of the red bands on the TL and CL. (C) Peak areas of the red bands on the TL. (D) A truth table of the "OR" logic gate. The concentrations of CEA and c-DNA are 200 ng mL^{-1} and 1 μM (Figs. S1 and S2, Supporting information), respectively. (For interpretation of the references to color in this figure legend, the reader is referred to the web version of this article.)

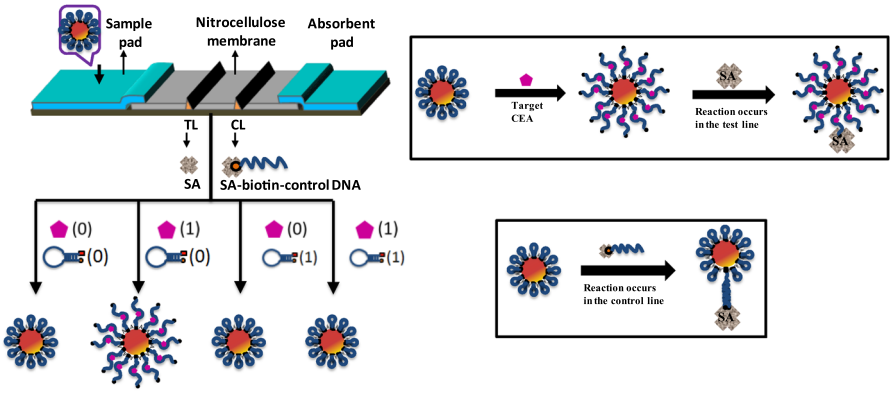

Scheme 3. Schematic illustration of the design strategy of the strip "INH" logic gate using CEA and HO-CEA as inputs.

3.3. *Design strategy of the strip "INH" logic gate*

In accordance with the conformation change of the HO, our system can also be used to design an "INH" logic gate with a slight change (Scheme 3). CEA and CEA-HO are the two inputs, with the absence and presence of each substance defined as "0" and "1", respectively. The output is the color of the test line, with the absence and presence of a red band on the test line defined as "0" and "1", respectively. Streptavidin and streptavidin–biotin–control DNA (partially complementary to the loop sequences of HO) were dispensed onto the nitrocellulose membrane to form the respective test and control lines. In the presence of (0,0) or (0,1) gate, which is in the absence of CEA, there was no compound formed by the CEA and CEA-HO in the sample solution, the hairpin structure remained contributing the biotin still masked by the AuNP; therefore, no AuNP conjugate was captured on the test line of the LFSB, and no red band was observed in the test line. In the presence of (1,1) state, which is in the presence of both CEA and CEA-HO in the sample solution, enough CEA-HO will combine with CEA protein to form a relatively stable compound; consequently there was no CEA protein to interact with CEA-HO self-assembling on the AuNP surface and the biotin still masked by the AuNP, and also no red band was observed in the test line. Only when in the presence of the CEA and in the absence of the CEA-HO, in the (1,0) state, CEA interact with CEA-HO self-assembling on the AuNP surface and the stems of HO open, leading to the biotin group "active". AuNPs associated with the activated biotins are captured on the test line of LFSB by preimmobilized streptavidin and there is a red band in the test line.

Part A of Fig. 2 illustrates representative photo images of the "INH" gate, part B highlights corresponding peak height of the test line and control line, part C lays out corresponding peak area of the test line. Only when the logic circuit was employed to the (1,0) state, there is a red band on the test line, in the mean time, the peak heights are much higher and the peak areas are much larger than other input combinations. The results are concluded in a truth table in part D.

The integration of "OR" and "INH" logic gates provided an approach for logic sensing applications where multiple target molecules were present. If there is no red band on the test line of

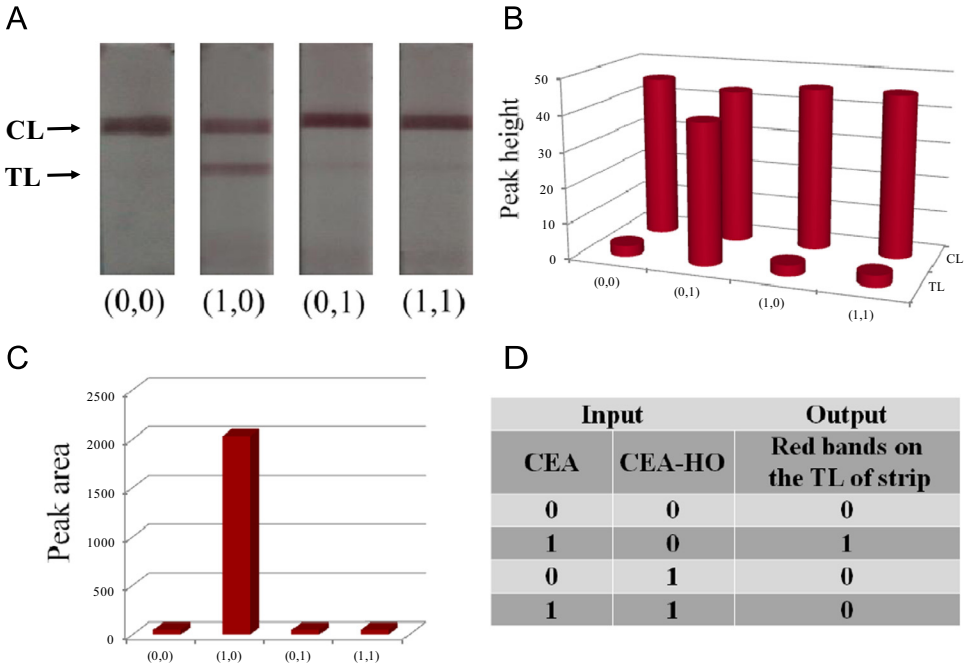

Input		Output
CEA	CEA-HO	Red bands on the TL of strip
0	0	0
1	0	1
0	1	0
1	1	0

Fig. 2. (A) Photo image of the LFSB in "INH" gate. (B) Peak height of the red bands on the TL and CL. (C) Peak areas of the red bands on the TL. (D) A truth table of the "INH" logic gate. The concentrations of CEA and CEA-HO are 200 ng mL^{-1} and 1 μM (Figs. S1 and S3, Supporting information), respectively. (For interpretation of the references to color in this figure legend, the reader is referred to the web version of this article.)

the "OR" or "INH" test strips, we could draw a conclusion that there was no target (neither CEA nor c-DNA) in the sample solution. If there is a red band on the test line of the "OR" test strip and no red band on the test line of the "INH" test strip, we could draw a conclusion that there is only c-DNA in the sample solution. If there is a red band on the test line of both the "OR" and "INH" test strip, we could draw a conclusion that there is CEA in the sample solution. This proof of concept might provide a new approach for multiplex analysis and nanobiomedical devices responding to multiple input chemicals.

3.4. The selectivity of the logic strips

In order to ensure the specificity of the system, in the "OR" logic gates, nontarget molecules such as myoglobin (MYO), mucoprotein (MUC), 1m-DNA and 3m-DNA functioned as negative control inputs. In the "INH" logic gates, OTA-HO and DNA-HO were applied as negative controls. As demonstrated in Fig. S4 (Supporting information), in the "OR" logic gate, only when CEA or c-DNA was utilized as stimulus input, a red band could be observed on the test line (output=1) compared with any of the control inputs. Referring to Fig. S5, the "INH" logic gate yielded no red band on the test line (output=1) in the presence of CEA as the first input and CEA-HO as the second input, but red band was observed on the test line (output=0) in the presence of other input as the second input. Such results indicate that the logic gates based on conformation change of the HO has good selectivity.

3.5. The practical applications of the logic strips

To demonstrate the feasibility of the proposed logic system for practical applications, "OR" and "INH" logic gates were operated in human serum samples. Serum samples were collected by diluting human serum to 10% in dilution buffer (20 mM Tris–HCl, 100 mM NaCl, 5 mM $MgCl_2$, pH 7.4). A sample solution containing the targets and HO was incubated for 30 min at room temperature and then applied to the sample pad of the LFSB for logic analysis. Fig. S6 exhibited, a red band appeared on the test zone (output=1) in the "OR" logic gate using CEA and/or c-DNA spiked in 10% human serum as inputs, but no red band was obtained when there was neither CEA nor c-DNA in serum sample. In Fig. S7, a red band is observed on the test line only when the "INH" gate is employed to the spiked CEA input (1,0). The other three combinations of inputs all lead to no red band on the test line. The results demonstrate the robustness of this strip logic system, which performs well even in relatively complex sample matrixes.

4. Conclusions

In the present work, we have demonstrated a universal strip system for proteins and DNAs based on a HO-functionalized AuNP system and LFSB with high specificity and sensitivity. The strategy depends on the unique molecular recognition properties of HO to proteins and DNAs to generate different quantities of "active" biotin groups on the AuNP surface. For further study, two logic gates ("OR" and "INH") were designed. CEA and c-DNA as inputs, gold nanoparticles as a tracer, the outputs can be directly visualized by observing the red bands on the test line of the strips. Such a logic gate system owns several unusual superiorities: (1) The unique stem–loop structure of hairpin DNA aptamer provides high specificity and offers the simple, rapid, and sensitive detection of any proteins and DNAs in theory, which can be used to seek potential substrate for multilevel logic gates and affords a path to the practical realization of a new generation of computers. (2) The biosensor is easy to use, no highly trained personnel or complicated instrumentation are needed. The logic operation with a user-friendly format is facilely fulfilled in laboratories. (3) The strip outputs can be explicitly judged by the presence or the absence of evident red bands on the test line, and each measurement can be readily finished within 10 min, which can be developed to a portable assay at ambient temperature. (4) The logic strips are revealed excellent selectivity and are capable of detecting targets in human serum solutions, illuminating the potential application of the logic design in clinical diagnostics. On account of these advantages, our work not only provides a visual and sensitive

detection method of proteins and DNAs but also presents a universal logic designing system for point-of-care and in-field diagnostics.

Acknowledgments

This work was supported by the National Natural Science Foundation of China (Nos. 21175032, 21275062) and the Natural Science Fund for Creative Research Groups of Hubei Province of China (No. 2011CDA111).

Appendix A. Supporting information

Supplementary data associated with this article can be found in the online version at 10.1016/j.bios.2014.06.007.

References

Andreasson, J., Pischel, U., 2010. Chem. Soc. Rev. 39, 174–188.
Chen, J., Fang, Z., Lie, P., Zeng, L., 2012. Anal. Chem. 84, 6321–6325.
Chen, X., Wang, Y., Liu, Q., Zhang, Z., Fan, C., He, L., 2006. Angew. Chem. Int. Ed. 45, 1759–1762.
Du, D., Wang, J., Wang, L., Lu, D., Lin, Y., 2012. Anal. Chem. 84, 1380–1385.
Ellington, A.D., Szostak, J.W., 1990. Nature 346, 818–822.
Fang, Z., Ge, C., Zhang, W., Lie, P., Zeng, L., 2011. Biosens. Bioelectron. 27, 192–196.
Fang, Z., Huang, J., Lie, P., Xiao, Z., Ouyang, C., Wu, Q., Wu, Y., Liu, G., Zeng, L., 2010. Chem. Commun. 46, 9043–9045.
Ge, C., Yu, L., Fang, Z., Zeng, L., 2013. Anal. Chem. 85, 9343–9349.
Halámková, L., Halámek, J., Bocharova, V., Wolf, S., Mulier, K.E., Beilman, G., Wang, J., Katz, E., 2012. Analyst 137, 1768–1770.
He, Y., Zeng, K., Gurung, A.S., Baloda, M., Xu, H., Zhang, X., Liu, G., 2010. Anal. Chem. 82, 7169–7177.
He, Y., Zhang, X., Zhang, S., Kris, M.K.L., Man, F.C., Kawde, A., Liu, G., 2012. Biosens. Bioelectron. 34, 37–43.
Katz, E., Privman, V., 2010. Chem. Soc. Rev. 39, 1835–1857.
Kim, D., Lynch, V.M., Park, J., Sessler, J.L., 2013. J. Am. Chem. Soc. 135 (39), 14889–14894.
Li, J., Yan, H., Wang, K., Tan, W., Zhou, X., 2007. Anal. Chem. 79, 1050–1056.
Lie, P., Liu, J., Fang, Z., Dun, B., Zeng, L., 2012. Chem. Commun. 48, 236–238.
Lin, Y., Tao, Y., Pu, F., Ren, J., Qu, X., 2011. Adv. Funct. Mater. 21, 4565–4572.
Liu, C., Jia, Q., Yang, C., Qiao, R., Jing, L., Wang, L., Xu, C., Gao, M., 2011. Anal. Chem. 83, 6778–6784.
Liu, G., Mao, X., Phillips, J.A., Xu, H., Tan, W., Zeng, L., 2009. Anal. Chem. 81, 10013–10018.
Liu, J., Chen, L., Lie, P., Dun, B., Zeng, L., 2013. Chem. Commun. 49, 5165–5167.
Liu, X., Aizen, R., Freeman, R., Yehezkeli, O., Willner, I., 2012. ACS Nano 6, 3553–3563.
Liu, Z., Zhang, W., Hu, L., Li, H., Zhu, S., Xu, G., 2010. Chem. Eur. J. 16, 13356–13359.
Lu, Y., Liu, Y., Zhang, S., Wang, S., Zhang, S., Zhang, X., 2013. Anal. Chem. 85, 6571–6574.
Mao, X., Ma, Y., Zhang, A., Zhang, L., Zeng, L., Liu, G., 2009. Anal. Chem. 81, 1660–1668.
Niu, Y., Zhao, Y., Fan, A., 2011. Anal. Chem. 83, 7500–7506.
Pan, J., Zhang, H., Cha, T., Chen, H., Choi, J.H., 2013. Anal. Chem. 85 (17), 8391–8396.
Pu, F., Ren, J., Yang, X., Qu, X., 2011a. Chem. Eur. J. 17, 9590–9594.
Pu, F., Liu, Z., Yang, X., Ren, J., Qu, X., 2011b. Chem. Commun. 47, 6024–6026.
Tuerk, C., Gold, L., 1990. Science 249, 505–510.
Vinkenborg, J.L., Karnowski, N., Famulok, M., 2011. Nat. Chem. Biol. 7, 519–527.
Wang, D., Fu, Y., Yan, J., Zhao, B., Dai, B., Chao, J., Liu, H., He, D., Zhang, Y., Fan, C., Song, S., 2014. Anal. Chem. 86 (4), 1932–1936.
Wang, L., Chen, W., Ma, W., Liu, L., Ma, W., Zhao, Y., Zhu, Y., Xu, L., Kuang, H., Xu, C., 2011. Chem. Commun. 47, 1574–1576.
Wang, Y., Li, C., Li, X., Li, Y., Kraatz, H., 2008. Anal. Chem. 80, 2255–2260.
Wang, L., Zhu, J., Han, L., Jin, L., Zhu, C., Wang, E., Dong, S., 2012. ACS Nano 6 (8), 6659–6666.
Xu, Z., Sato, Y., Nishizawa, S., Teramae, N., 2009. Chem. Eur. J. 15, 10375–10378.
Yoshida, W., Yokobayashi, Y., 2007. Chem. Commun. 2, 195–197.
Zhang, J., Chen, C., Xu, X., Wang, X., Yang, X., 2013. Chem. Commun. 49, 2691–2693.
Zhang, J., Wang, L., Pan, D., Song, S., Boey, F.Y.C., Zhang, H., Fan, C., 2008. Small 4, 1196–1200.
Zhang, L., Zhang, Y., Liang, R., Qiu, J., 2013. J. Phys. Chem. C 117 (23), 12352–12357.
Zhang, Y., Tang, Z., Wang, J., Wu, H., Maham, A., Lin, Y., 2010. Anal. Chem. 82, 6440–6446.